

Journal of Materials Chemistry A

Accepted Manuscript



This is an *Accepted Manuscript*, which has been through the Royal Society of Chemistry peer review process and has been accepted for publication.

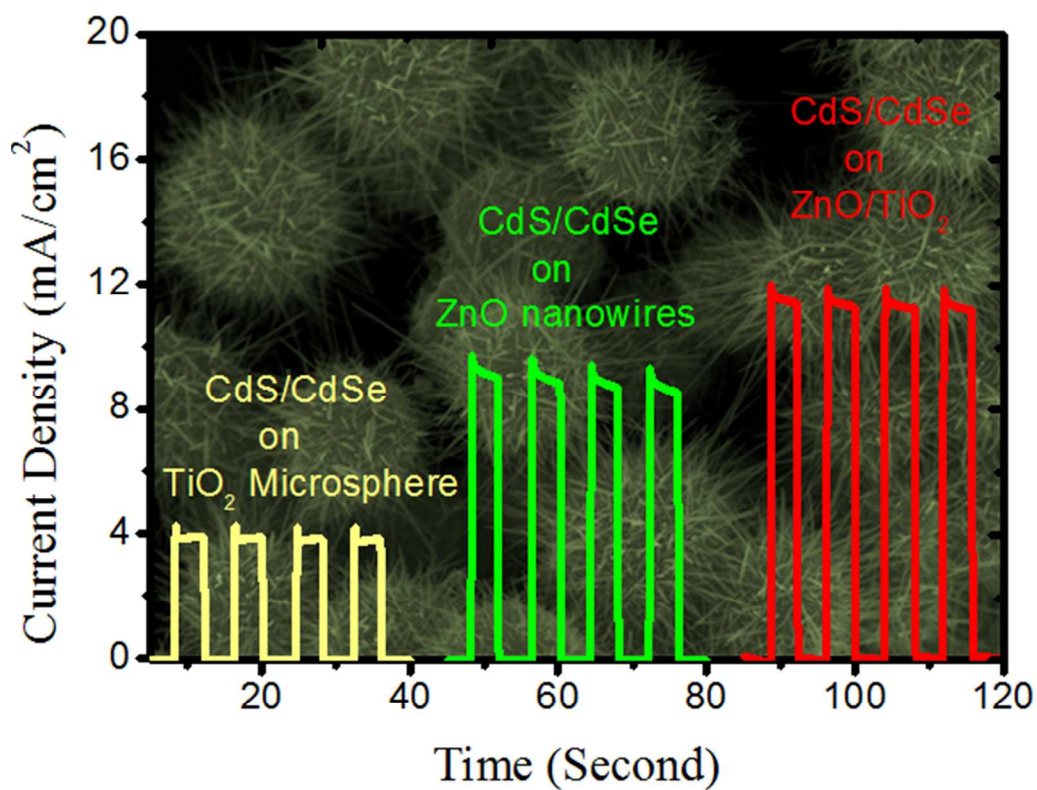
Accepted Manuscripts are published online shortly after acceptance, before technical editing, formatting and proof reading. Using this free service, authors can make their results available to the community, in citable form, before we publish the edited article. We will replace this *Accepted Manuscript* with the edited and formatted *Advance Article* as soon as it is available.

You can find more information about *Accepted Manuscripts* in the [Information for Authors](#).

Please note that technical editing may introduce minor changes to the text and/or graphics, which may alter content. The journal's standard [Terms & Conditions](#) and the [Ethical guidelines](#) still apply. In no event shall the Royal Society of Chemistry be held responsible for any errors or omissions in this *Accepted Manuscript* or any consequences arising from the use of any information it contains.

TOC

ZnO/TiO₂-based hybrid heterostructures co-sensitized with CdS and CdSe showed remarkable PEC response while offering efficient scattering of sunlight in the visible frequency domain, and efficient electron-hole separation and transport.



ARTICLE

Highly Efficient Photoelectrochemical Response by Sea-Urchin Shaped ZnO/TiO₂ Nano/Micro Hybrid Heterostructures Co-sensitized with CdS/CdSe

Cite this: DOI: 10.1039/x0xx00000x

Zahid Ali^{a,b}, Imran Shakir^a, and Dae Joon Kang^{a*}

Received 00th January 2012,

Accepted 00th January 2012

DOI: 10.1039/x0xx00000x

www.rsc.org/

Photoelectrochemical cells have existed for decades. However, the poor efficiency of such devices is still problematic because of trade-offs between different materials properties used for photoelectrochemical reactions. Here we report a novel photoanode architecture consisting of CdS/CdSe co-sensitized sea urchin-shaped ZnO/TiO₂-based nano/micro hybrid heterostructures that simultaneously offer better light scattering over the entire visible frequency domain, better separation of photo-generated charge carriers, significantly improved light absorption that extends over a broad visible spectrum, and better transport of electrons through a highly connected network of conducting ZnO nanowires than existing architectures. Use of the synthesized structures as photoanodes in a photoelectrochemical cell yielded a photocurrent density as high as 11.8 mA/cm² with a remarkable photo-conversion efficiency of 6.4 %.

Introduction

Photoelectrochemical (PEC) water splitting¹⁻⁴ is considered the holy grail of sustainable energy. Semiconductor materials with a band gap energy of 1.23 eV⁵ are ideal for splitting water, but kinetic and thermodynamic non-idealities in water redox reactions at the semiconductor-water interface demand significantly higher energy than 1.23 eV in practice, hence only wide band gap semiconductors have been effective thus far. Unfortunately, these large band gap semiconductors can absorb only 5% of the solar spectrum, which is the major obstacle in achieving good water splitting efficiencies.⁶⁻⁸ During the past few decades, considerable efforts have been devoted to improve the light absorption range of these photocatalysts. Among the various strategies suggested, sensitization of large band gap semiconductors (*i.e.* TiO₂, ZnO, WO₃) with narrow band gap semiconductors (*i.e.* CdS, CdSe, CdTe) appears to be a promising approach as it offers a) extended absorption of the solar spectrum in the visible frequency domain by using a narrow band gap semiconductor, b) the ability to tune the band level to a position suitable for water redox reactions via heterostructure formation and c) better separation of photo-generated charge carriers at heterojunction interfaces.⁹⁻¹¹

To exploit the synergistic effects that can be obtained by coupling large band gap and narrow band gap semiconductors, a purpose-designed architecture is essential to provide a large surface area, to improve electron transport, and to reduce minority carrier diffusion length and charge carrier recombination losses. Furthermore, increased optical path length is also highly desirable to maximize the absorption of visible photons in ultra-thin layers of narrow band gap semiconductors.¹² However, designing a material architecture with these properties is challenging because of trade-

offs between different materials properties; sensitization of large band gap semiconductors with narrow band gap semiconductors has to date only resulted in a marginal improvement in PEC response.^{13,14}

Herein, we report an innovative photoanode architecture that we developed using sea urchin-shaped ZnO/TiO₂-based nano/micro hybrid heterostructures co-sensitized with CdS and CdSe to simultaneously achieve a) efficient absorption of sunlight in the visible frequency domain, b) efficient scattering of sunlight in the visible frequency domain, and c) efficient electron-hole separation and transport. We investigated the microstructure and morphology of the synthesized structures by scanning electron microscopy, X-ray diffraction, and transmission electron microscopy. The synthesized structures showed a remarkable PEC response when used as photoanodes in a PEC cell.

Experimental

Synthesis: TiO₂ microspheres were synthesized by the sol-gel method.¹⁵ Four grams of hexadecylamine (90%, Sigma Aldrich, Korea) was dissolved in 400 mL of ethanol (99.99%, Sigma Aldrich, Korea) and 1.9 mL of 0.1 M KCl (AR, BDH) solution, followed by the addition of 9 mL of titanium isopropoxide (TTIP, 97%, Sigma Aldrich, Korea) under vigorous stirring. After keeping the solution static for 24 hours, the obtained spheres were subsequently washed three times, and dried at 50°C before calcination at 500°C. Annealed microspheres were then coated with ZnO by dispersing them in seed layer solution¹⁶ under a mild stirring condition for 8 hours. The methanol was evaporated at room temperature and the dried samples were heated at 150°C for 10 minutes to obtain ZnO nanocrystals on the surface of the microspheres. The process was repeated 2-3 times

to ensure full coverage of the microspheres with the ZnO seed layer. In the third step, coated spheres were dispersed in 20 mL of aqueous solution comprising 25 mM zinc nitrate hexahydrate, 25 mM hexamethylenetetramine (HMTA), and 5 mM polyethylene amine (PEI). The solution was kept in a sealed glass vessel and heated at 95°C in an oil bath under a mild stirring condition. The obtained core-shell structures were then centrifuged and washed three times before drying.

CdS/CdSe Sensitization and Photoanode Preparation: To synthesize CdS/CdSe co-sensitized ZnO/TiO₂ sea urchin structures, slurry was first prepared using the ZnO/TiO₂ hybrid heterostructures, ethyl cellulose, and ethanol. This slurry was then coated on FTO substrate glass (2.2 mm thick with 15 ohm/square sheet resistance, Solaronix, Switzerland) using a doctor-blade technique. Films were scratched into an area of 1 cm x 1 cm and then heat-treated at 300°C for 30 minutes. After heat treatment, films were sensitized with CdS and CdSe according to the procedure outline in reference.¹⁷ Briefly, heat-treated films were immersed in 0.1 M Na₂S (99.99%, Sigma Aldrich, Korea) aqueous solution prepared for 10 minutes at room temperature, which resulted in the formation of a thin ZnS layer on top of the ZnO nanowires grown on the TiO₂ microspheres that served as a leading layer for the formation of a CdS shell. After rinsing with DI water, films with ZnS as an outer layer were immersed in an aqueous solution of 0.025 M cadmium acetate (99.99%, Sigma Aldrich, Korea), 0.1 M thiourea (99%, Sigma Aldrich, Korea), and 0.1 M ethylenediamine (99.99%, Sigma Aldrich, Korea) for 1 hour at room temperature. After this process, films were again rinsed with DI water and finally immersed in a solution prepared by dissolving 15 mg of Se powder (99.99%, Sigma Aldrich, Korea) and 50 mg of NaBH₄ (98%, Sigma Aldrich, Korea) in 30 mL of DI water and kept at 90°C for 3 hours. After this process, films were washed and heat-treated at 300°C for 30 minutes.

Physical Characterization: Structural analysis of the samples was performed using X-ray diffractometry (XRD, Rigaku Rotaflex D/Max) with Cu K_α radiation (wavelength (λ) = 1.5418 Å) and field emission high-resolution transmission electron microscopy (FE-TEM, JEOL JEM-2100F, Japan). The morphology of the ZnO/TiO₂ heterostructures was determined by field emission scanning electron microscopy (FE-SEM, JEOL JSM – 7401F, Japan). Diffuse transmittance and total transmittance spectra were collected on a Cary 5000 UV-Vis-NIR spectrophotometer with an integrating sphere (Internal DRA-2500) accessory.

Photoelectrochemical Measurements: Photocurrent–potential responses (*I*–*V* curves) were recorded with a 150 W xenon lamp-based solar simulator (PECCELL, Yokohama, Japan, PECL01: 100 mW cm⁻²). Light intensity was calibrated using a silicon reference cell (Fraunhofer ISE, Certificate No. CISE269). The electrolyte comprised of an aqueous solution of 0.25M Na₂S and 0.35M Na₂SO₃ bubbled with nitrogen stream. Incident photon to current efficiency (IPCE) was measured using a 300 W xenon light source and a monochromator (Polaronix K3100 IPCE Measurement System, McScience, Korea) in conjunction with equation¹⁸

$$IPCE = \frac{(1240 \times I)}{(\lambda \times J_{light})}$$

where *I* is the photocurrent density, λ is the incident light wavelength, and *J*_{light} is the measured irradiance.

Results and Discussions

As-synthesized TiO₂ microspheres had a very smooth surface and a diameter of around 1 μm, as shown in Fig 1a. These spheres were calcined at 500°C, which resulted in a 33% reduction in the size of the microspheres as well as transformation from an amorphous to an anatase phase (see XRD pattern in supporting information Fig. S1). The inset in Fig. 1b shows a SEM image of spheres coated with a ZnO seed layer; ZnO nanocrystals can clearly be observed and the growth of ZnO nanowires from these nanocrystals after 1 hour of hydrothermal reaction is shown in Fig. 1b. A SEM image of the final sea urchin-shaped ZnO/TiO₂ heterostructures obtained after 4 hours of hydrothermal reaction under mild stirring conditions is shown in Fig. 1c. The diameter of the ZnO nanowires grown on the TiO₂ microspheres was around ~ 35 nm as indicated in Fig. 1d.

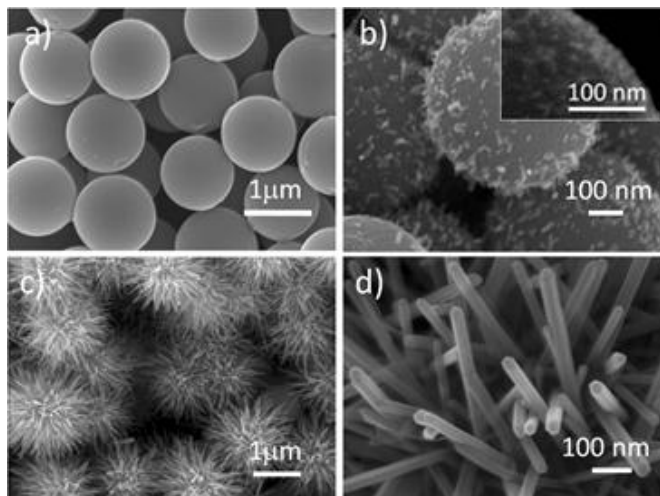


Fig. 1: (a) SEM images of as-synthesized TiO₂ microspheres, (b) TiO₂ microspheres coated with a ZnO seed layer, (c) ZnO/TiO₂ hybrid structures, and (d) ZnO nanowires grown on TiO₂ microspheres.

Finally, the ZnO/TiO₂-based sea urchin structures were sensitized with CdS and CdSe using the successive ionic layer adsorption and reaction (SILAR) method, and the structural properties of the synthesized structures were investigated by transmission electron microscopy. A high resolution transmission electron microscope HRTEM image and the selected area electron diffraction (SAED) pattern of single ZnO nanowires grown on TiO₂ microspheres are shown in Fig. 2a and the inset in Fig. 2a, respectively, indicating the single crystalline nature of the ZnO nanowires. A lattice spacing of 5.2 Å between adjacent lattice planes was observed from Fig. 2a, which corresponds to the distance

between two (0002) crystal planes of ZnO, confirming that the growth of the ZnO nanowires is along the [0001] direction. A HRTEM image of a single ZnO nanowire after CdS sensitization is shown in **Fig. 2b**; the measured lattice spacing of the core (0.52 nm) and shell layer (0.32 nm) are consistent with the *d*-spacing values of ZnO and CdS, respectively, confirming that the ZnO nanowires were uniformly covered with CdS nanocrystals with an average diameter of 3–10 nm. A TEM image of a CdS/ZnO core shell nanowire after CdSe sensitization is shown in **Fig. 2c**. It can be observed from this figure that the CdSe sensitization process resulted in the formation of nanocrystals on the surface of the CdS/ZnO core shell nanowire. The lattice spacing value for these nanocrystals was calculated to be 0.36 nm from the HRTEM image shown in **Fig. 2d**; this value is in agreement with the *d* spacing value for the (111) plane of CdSe.

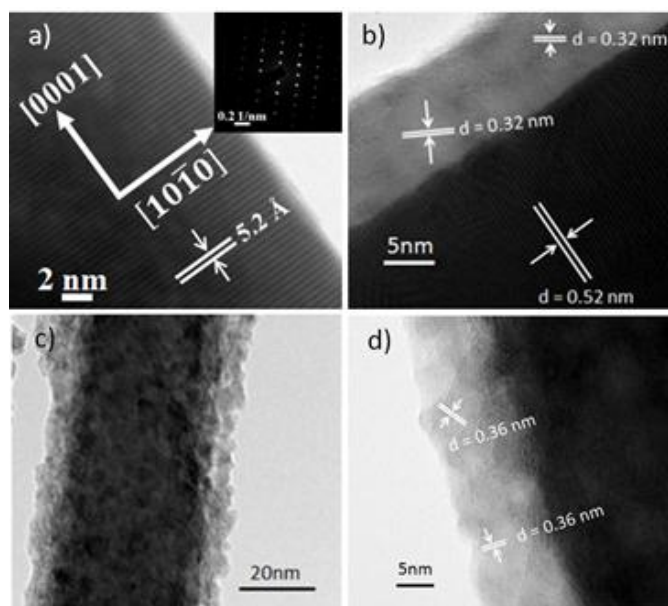


Fig. 2 a) HRTEM image of a ZnO nanowire (inset is the SAED pattern of the ZnO nanowire); b) HRTEM image of a CdS/ZnO core shell nanowire; c) TEM image of a CdS/ZnO core shell nanowire after CdSe Sensitization; and d) HRTEM image of part of the nanowire shown in **Fig. 2c**.

To further verify the presence of CdS and CdSe on the ZnO nanowires, we performed energy-dispersive X-ray spectroscopy (EDX) elemental mapping of individual CdS/CdSe-sensitized ZnO nanowires grown on TiO₂ microspheres and the results are shown in **Fig. 3a**. The corresponding elemental maps of Zn, O, Cd, S, and Se are shown in **Figs. 3b - 3f**, respectively, and demonstrate the uniform distribution of CdS and CdSe on the surface of the ZnO nanowires. EDX elemental mapping confirmed an approximate atomic ratio of 65:35 for S and Se in the CdS/CdSe co-sensitized ZnO nanowires.

ZnO/TiO₂-based sea urchin structures were purposely designed to have superior optical properties. The size of TiO₂ microspheres suitable for scattering light over the entire visible range was calculated using Mie scattering theory, which predicts the effective electric and/or magnetic polarizability densities of

scattering objects.^{19, 20} Light scattering by a spherical particle much smaller than the incident light wavelength can be accurately determined by the Mie solution. The scattered field of a single dielectric sphere with radius *r*₀ and relative refractive index *n* can be decomposed into a multipole series. The 2^m-pole term of the scattered electric field is proportional to

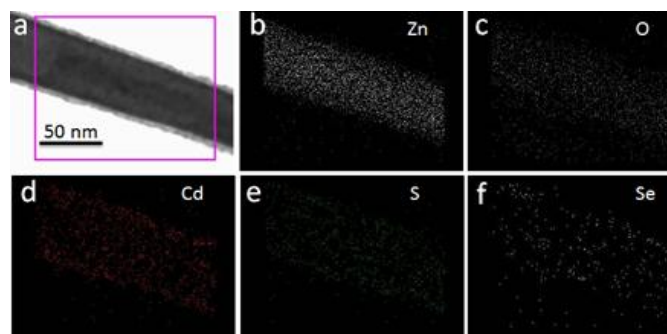


Fig. 3 a) TEM image of a CdSe/CdS/ZnO core shell nanowire; b) TEM elemental map for Zn; c) TEM elemental map for O; d) TEM elemental map for Cd; e) TEM elemental map for S; and f) TEM elemental map for Se.

$$a_m = \frac{n\psi_m(nka)\psi'_m(ka) - \psi_m(ka)\psi'_m(nka)}{n\psi_m(nka)\xi'_m(ka) - \xi'_m(x)\psi'_m(nka)}$$

while the 2^m-pole term of the scattered magnetic field is proportional to

$$b_m = \frac{\psi_m(nka)\psi'_m(ka) - n\psi_m(ka)\psi'_m(nka)}{\psi_m(nka)\xi'_m(ka) - n\xi'_m(ka)\psi'_m(nka)}$$

where *k* is the wave vector, *a* is the sphere radius, *n* is the refractive index of the material, ψ_m is an *m*th order Bessel function of the first kind, and ξ_m is an *m*th order Hankel function of the first kind. The prime indicates the derivative with respect to the argument. Only the *a*₁ and *b*₁ coefficients, which are the strength of the electric and magnetic dipole responses, are used to calculate scattering efficiency.²¹ We used the equation shown below to calculate the scattering efficiency of TiO₂ spherical particles:

$$Q_s = \frac{2}{x^2} \sum_{n=1}^{\infty} (2n+1)(|a_n|^2 + |b_n|^2)$$

where *Q_s* represents the light scattering efficiency.

Our theoretical calculation revealed that TiO₂ particles with a diameter of ~ 0.8 μm are required for light scattering in the visible frequency domain. However, keeping in mind that micron-size particles offer less surface area than nano-sized particles, we grew vertical ZnO nanowires on the surfaces of TiO₂ microspheres to

increase surface area. These vertical ZnO nanowires also provided a conducting channel for electron transport and improved the adhesion of the CdS layer by the formation of ZnS as a gluing layer during the CdS/CdSe sensitization process.

Light scattering response of ZnO/TiO₂ based sea urchin structures was experimentally calculated as a percentage haze value (see Fig. 4a) from the diffused transmittance and total transmittance spectra (Fig. S2 supporting information) according to the following equation²²⁻²⁴

$$\text{Haze Value (\%)} = \frac{\text{Diffuse Transmittance}}{\text{Total transmittance}} \times 100$$

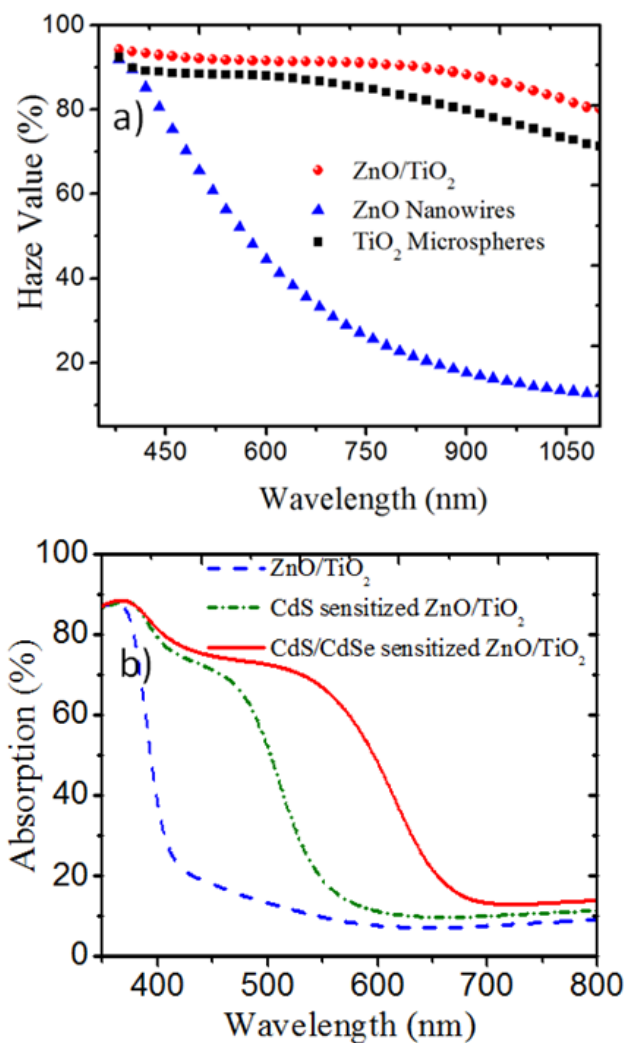


Fig. 4. a) Percentage haze value for TiO₂ microspheres, ZnO nanowires and the ZnO/TiO₂ sea urchin b) Absorption spectra of ZnO/TiO₂ sea urchin CdS, and CdS/CdSe sensitized ZnO/TiO₂ sea urchin structure.

The spectral dependence of the haze value was compared to that of ZnO nanowires and TiO₂ microspheres. A significant improvement in response was observed in the entire visible wavelength range, as shown in Fig. 4a. Once we had synthesized

structure which can scatter light in the entire visible range, it was then sensitized with CdS and CdSe to efficiently absorb visible photons. After sensitization with CdS and CdSe, we performed UV-Vis and the results were plotted as in Fig. 4b. It can be observed from Fig. 4b that the absorption edge for ZnO/TiO₂ sea urchin structure is in the UV region at wavelengths around 400 nm while after sensitization with CdS or CdSe, absorption range was significantly extended in the visible frequency domain. The degree of red shift after CdS/CdSe co-sensitization was larger than that of CdS sensitized ZnO/TiO₂ sea urchin structure which can be attributed to the smaller band gap of CdSe as compared to CdS.

Another advantage of synthesized cascade structure was the stepwise position of band edges due the redistribution of electrons between CdS and CdSe in order to align Fermi levels.²⁵ This stepwise structure of the band edges as shown Fig. 5a is not only suitable for the efficient injection photo-excited electron but also advantageous for hole-recovery in both CdS and CdSe layers and hence could improve the PEC response when exploited as photoanode for PEC cells. To evaluate the potential of CdS/CdSe sensitized ZnO/TiO₂ heterostructure as photoanode, we performed photoelectrochemical measurements under dark and simulated sunlight irradiation (AM 1.5, 100mW/cm²). Fig. 5b shows a set of linear sweep voltammograms recorded for the ZnO/TiO₂, CdS sensitized ZnO/TiO₂ and CdS/CdSe sensitized ZnO/TiO₂ based photoanodes. Dark current density for all the samples was in the range of 10⁻¹ to 10⁻³ mA/cm² from -1.3 to 0.5 V vs. Ag/AgCl. It can be observed from Fig. 5b that after sensitization with CdS and CdS/CdSe the photoanodes showed substantially enhanced photo response as compared to bare ZnO/TiO₂ based photoanode. It is worth noting that CdS/CdSe co-sensitized ZnO/TiO₂ structure have shown a photocurrent density of ~11.8 mA/cm² at 0.4 V, which is about two times larger than that of CdS sensitized ZnO/TiO₂ based photoanode. In order to evaluate the role of ZnO/TiO₂ heterostructure we compared photoelectrochemical response of CdS/CdSe sensitized ZnO/TiO₂ based photoanodes to that of CdS/CdSe sensitized ZnO nanowires and CdS/CdSe sensitized TiO₂ microsphere based photoanode as shown in Fig. 6a. It can be observed from Fig. 6a that CdS/CdSe sensitized TiO₂ microsphere based photoanode has delivered only 3mA/cm², whereas CdS/CdSe sensitized ZnO nanowires and CdS/CdSe sensitized ZnO/TiO₂ based photoanode have shown a photocurrent density of 8mA/cm² and 11 mA/cm² respectively at an applied bias potential of 0.4V. The higher photoelectrochemical response of ZnO nanowires can be attributed to better adhesion of CdS on ZnO as in the case of ZnO nanowire formation of a ZnS layer that functioned as glue for the CdS layer, the high electronic conductivity of ZnO nanowires, and their high surface area. Further improvements in the photoresponse of the CdS/CdSe-sensitized ZnO/TiO₂ sea urchin structures is solely due to the better higher light scattering offered by the ZnO/TiO₂ sea urchin structures; these structures significantly improved the optical path length by multiscattering, allowing efficient absorption of a broader spectrum of sunlight by the thin CdS/CdSe shells around the ZnO nanowires.

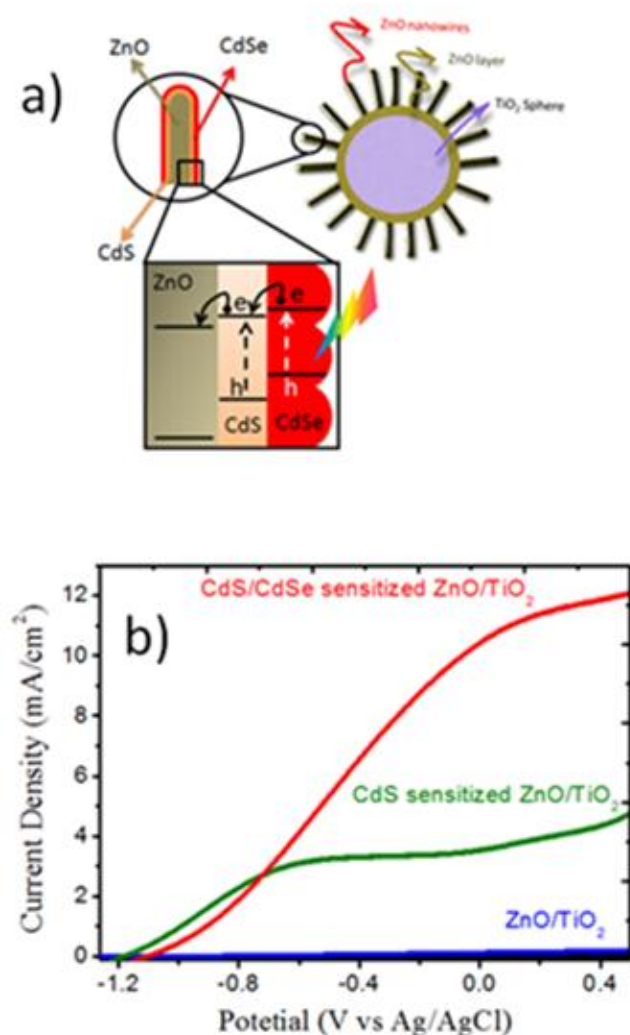


Fig. 5. a) Proposed band diagram for the CdS/CdSe co-sensitized ZnO/TiO₂ sea urchin structures; b) linear sweep voltammograms for the ZnO/TiO₂ sea urchin structures, CdS-sensitized ZnO/TiO₂ sea urchin structures, and CdS/CdSe co-sensitized ZnO/TiO₂ sea urchin structures.

The efficiency (η) of water splitting of photoelectrochemical cells equipped with ZnO/TiO₂ sea urchin structures, CdS-sensitized ZnO/TiO₂ sea urchin structures, and CdS/CdSe co-sensitized ZnO/TiO₂ sea urchin structures under an applied voltage was calculated according to the following equation²⁶

$$\eta = \frac{I(1.23 - V_{app})}{P_{light}}$$

where V_{app} is the applied voltage versus RHE, I is the externally measured current density, and P_{light} is the power density of illumination. The PEC efficiencies of ZnO/TiO₂, CdS-sensitized ZnO/TiO₂, and CdS/CdSe co-sensitized ZnO/TiO₂ are compared in **Fig. 6b**. The photo-conversion efficiency of the CdS/CdSe-sensitized ZnO/TiO₂-based photoanode was significantly higher than

that of the CdS-sensitized ZnO/TiO₂ photoanode. Our PEC results clearly demonstrate the unique benefits of CdS/CdSe co-sensitized ZnO/TiO₂-based photoanodes; these can efficiently harvest sunlight in the visible frequency domain due to the smaller band gap of CdS and CdSe than ZnO and yield better separation of photo-generated charge carriers due to the stepwise structure of band edges in CdSe/CdS/ZnO.

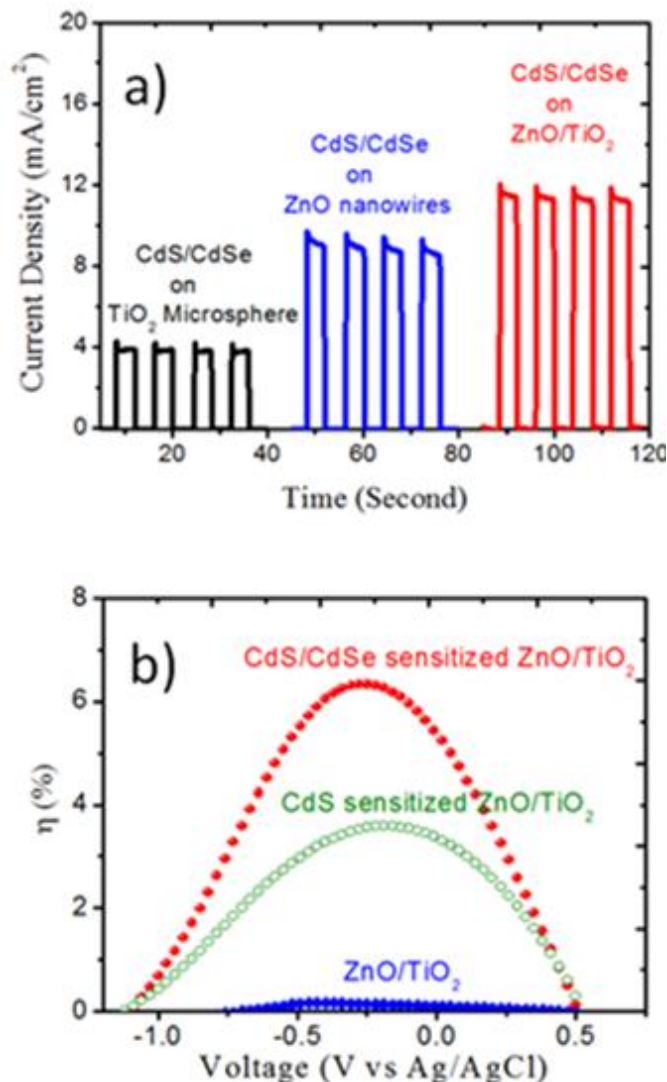


Fig. 6. a) Amperometric I-t curves for CdS/CdSe co-sensitized ZnO/TiO₂ sea urchin structures, CdS/CdSe co-sensitized ZnO nanowires, and CdS/CdSe co-sensitized TiO₂ microspheres; b) PEC efficiency of ZnO/TiO₂ sea urchin structures, CdS-sensitized ZnO/TiO₂ sea urchin structures, and CdS/CdSe co-sensitized ZnO/TiO₂ sea urchin structures.

Conclusions

We successfully designed novel photoanodes for PEC cell based on CdS/CdSe co-sensitized ZnO/TiO₂ sea urchin structures synthesized via combined sol-gel and hydrothermal processes. The sea urchin structures had a dramatically enhanced optical path length due to

multi-scattering allowing efficient absorption of a broader spectrum of sunlight, and showed good separation of photo-generated charge carriers due to the stepwise structure of the band edge positions and improved electronic transport through the conducting ZnO nanowires. A promising photocurrent density of 11.8 mA/cm² was achieved at an applied bias voltage of 0.4 V under simulated sunlight irradiation, corresponding to an overall photo conversion efficiency of 6.4%.

Acknowledgements

This work was supported by Center for BioNano Health-Guard funded by the Ministry of Science, ICT & Future Planning (MSIP) of Korea as Global Frontier Project (H-GUARD_2013M3A6B2078944) and Basic Science Research Program through the National Research Foundation of Korea (NRF) funded by the Ministry of Education (S-2011-0292-000).

Notes and references

^a Department of Physics, Institute of Basic Sciences, Sungkyunkwan University, Suwon 440-746, Republic of Korea

^b National Institute of Lasers and Optronics, Islamabad, Pakistan

* to whom correspondence should be addressed: djkgang@skku.edu

Electronic Supplementary Information (ESI) available: [XRD spectra of TiO₂ microspheres and ZnO/TiO₂ nano/micro hybrid heterostructures, diffuse and total transmittance spectra of TiO₂ microspheres, ZnO nanowires, and ZnO/TiO₂ sea urchin structures]. See DOI: 10.1039/b000000x/

1. S. U. M. Khan, M. Al-Shahry and W. B. Ingler, *Science*, 2002, **297**, 2243-2245.
2. X. Zhang, F. Wang, H. Huang, H. Li, X. Han, Y. Liu and Z. Kang, *Nanoscale*, 2013, **5**, 2274-2278.
3. P. A. DeSario, J. J. Pietron, D. E. DeVantier, T. H. Brintlinger, R. M. Stroud and D. R. Rolison, *Nanoscale*, 2013, **5**, 8073-8083.
4. S. Hoang, S. Guo and C. B. Mullins, *The Journal of Physical Chemistry C*, 2012, **116**, 23283-23290.
5. B. Jeremie, Y. Jun-Ho, C. Maurin, H. Takashi, S. Renata, A. Jan, G. Michael and S. Kevin, *Nature Photonics*, 2012, **6**, 824-828.
6. M. Ni, M. K. H. Leung, D. Y. C. Leung and K. Sumathy, *Renewable and Sustainable Energy Reviews*, 2007, **11**, 401-425.
7. F. Su, T. Wang, R. Lv, J. Zhang, P. Zhang, J. Lu and J. Gong, *Nanoscale*, 2013, **5**, 9001-9009.
8. K. Maeda and K. Domen, *The Journal of Physical Chemistry Letters*, 2010, **1**, 2655-2661.
9. H. Park, W. Choi and M. R. Hoffmann, *Journal of Materials Chemistry*, 2008, **18**, 2379-2385.
10. H. M. Chen, C. K. Chen, R.-S. Liu, L. Zhang, J. Zhang and D. P. Wilkinson, *Chemical Society Reviews*, 2012, **41**, 5654-5671.
11. H. Kim, M. Seol, J. Lee and K. Yong, *The Journal of Physical Chemistry C*, 2011, **115**, 25429-25436.
12. G. Wang, X. Yang, F. Qian, J. Z. Zhang and Y. Li, *Nano Letters*, 2010, **10**, 1088-1092.
13. C.-J. Lin, Y.-T. Lu, C.-H. Hsieh and S.-H. Chien, *Applied Physics Letters*, 2009, **94**, 113102-113103.
14. Y. Horiuchi, T. Toyao, M. Takeuchi, M. Matsuoka and M. Anpo, *Physical Chemistry Chemical Physics*, 2013, **15**, 13243-13253.

15. D. Chen, L. Cao, F. Huang, P. Imperia, Y.-B. Cheng and R. A. Caruso, *Journal of the American Chemical Society*, 2010, **132**, 4438-4444.
16. C. Pacholski, A. Kornowski and H. Weller, *Angewandte Chemie International Edition*, 2002, **41**, 1188-1191.
17. Z. Lu, J. Xu, X. Xie, H. Wang, C. Wang, S.-Y. Kwok, T. Wong, H. L. Kwong, I. Bello, C.-S. Lee, S.-T. Lee and W. Zhang, *The Journal of Physical Chemistry C*, 2011, **116**, 2656-2661.
18. A. B. Murphy, P. R. F. Barnes, L. K. Randeniya, I. C. Plumb, I. E. Grey, M. D. Horne and J. A. Glasscock, *International Journal of Hydrogen Energy*, 2006, **31**, 1999-2017.
19. J. Taylor, *Optical Binding Phenomena: Observations and Mechanisms*; Springer Berlin Heidelberg: 2011, p 11.
20. Z. Zhang and S. Satpathy, *Physical Review Letters*, 1990, **65**, 2650-2653.
21. J. A. Schuller, R. Zia, T. Taubner and M. L. Brongersma, *Physical Review Letters*, 2007, **99**, 107401.
22. T. Nonami, H. Taoda, N. T. Hue, E. Watanabe, K. Iseda, M. Tazawa and M. Fukaya, *Materials Research Bulletin*, 1998, **33**, 125-131.
23. H. Stiebig, N. Senoussaoui, C. Zahren, C. Haase and J. Müller, *Progress in Photovoltaics: Research and Applications*, 2006, **14**, 13-24.
24. N. Intawiwat, E. Myhre, H. Øysæd, S. H. Jamtvedt and M. K. Pettersen, *Polymer Engineering & Science*, 2012, **52**, 2015-2024.
25. Y.-L. Lee and Y.-S. Lo, *Advanced Functional Materials*, 2009, **19**, 604-609.
26. Y. Lei, G. Zhao, M. Liu, Z. Zhang, X. Tong and T. Cao, *The Journal of Physical Chemistry C*, 2009, **113**, 19067-19076.